Ocean Sci., 8, 333–344, 2012
www.ocean-sci.net/8/333/2012/
doi:10.5194/os-8-333-2012

Ocean Science

Transports and budgets in a 1/4 ° global ocean reanalysis 1989–2010

K. Haines, M. Valdivieso, H. Zuo, and V. N. Stepanov

ESSC and Dept. of Meteorology, University of Reading, Reading, RG6 6AL, UK

Correspondence to: K. Haines (k.haines@reading.ac.uk)

Received: 27 December 2011 – Published in Ocean Sci. Discuss.: 23 January 2012
Revised: 19 April 2012 – Accepted: 27 April 2012 – Published: 7 June 2012

Abstract. Large-scale ocean transports of heat and freshwater have not been well monitored, and yet the regional budgets of these quantities are important to understanding the role of the oceans in climate and climate change. In contrast, atmospheric heat and freshwater transports are commonly assessed from atmospheric reanalysis products, despite the presence of non-conserving data assimilation based on the wealth of distributed atmospheric observations as constraints. The ability to carry out ocean reanalyses globally at eddy-permitting resolutions of 1/4 ° or better, along with new global ocean observation programs, now makes a similar approach viable for the ocean. In this paper we examine the budgets and transports within a global high resolution ocean model constrained by ocean data assimilation, and compare them with independent oceanic and atmospheric estimates.

1 Introduction

Ocean reanalyses or ocean syntheses have the potential to provide useful, complete, time-evolving descriptions of the ocean state, and particularly the ocean circulation, which cannot be obtained in any other way, given the disparate and asynoptic nature of the ocean observational data sets. In the atmosphere, reanalysis activities have become of great importance to research, and it has become commonplace to use atmospheric wind patterns from reanalysis products to investigate regional phenomena and processes, e.g. heat, water vapour or chemical transports. In the oceans, the scarcity of historical observational data, coupled with a plethora of research mode numerical models, has meant that there are many more ocean circulation products available. A recent summary of the state of the art in developing ocean synthesis products can be found in Stammer et al. (2010). The vast majority of global synthesis products have been based on using lower resolution numerical models, often to permit the application of more sophisticated data assimilation approaches. The simple ocean data assimilation (SODA) system of Carton and Giese (2008) and Zheng and Giese (2009) is the most similar in design to the work being presented here.

In this paper we report on a global 1/4 ° by 46-level ocean reanalysis product developed as part of the EU GMES Marine Service project MyOcean. The entire period of the reanalysis covers 1989–2010, but we report primarily on the period 1993–2009, as the MyOcean project is developing an intercomparison of ocean products for this period. The standard evaluations of this reanalysis product against the observational data being assimilated, or against independent but related products to the observations are available through the MyOcean product reports (Valdivieso et al., 2011a, b). In this paper we focus on using the reanalysis product to assess transports for heat and freshwater, both in terms of exchanges at the ocean surface with the atmosphere, and horizontal transports within the oceans. We develop closed budgets for heat and freshwater exchanges both globally and within ocean basins, where the role of ocean data assimilation is explicitly resolved and interpreted.

In Sect. 2 we describe the model, the surface forcing, and the data assimilation process. In Sect. 3 we look at the global and regional heat budgets within the reanalysis product. In Sect. 4 we do the same for the freshwater budgets. In Sect. 5 we put a particular focus on the meridional overturning circulation (MOC) in the Atlantic Ocean and the meridional heat and freshwater transports in that basin. Section 6 is a summary and conclusions.

Published by Copernicus Publications on behalf of the European Geosciences Union.

2 Model and data assimilation description

2.1 Ocean model

The numerical model used is the NEMO coupled ice-ocean model(Madec, 2008) version 2.3, based on the OPA9 ocean model (Madec et al., 1998) and the LIM2.0 sea ice model (Louvain sea ice model: Fichefet and Maqueda, 1997; Goosse and Fichefet, 1999). It is a primitive equation z-level model with hydrostatic and Boussinesq approximations, and a free surface (Roullet and Madec, 2000) with partial cell topography (Adcroft et al., 1997). It has the tri-polar "ORCA" 1/4° grid and 46 levels with thicknesses from 6–250 m, as developed through the DRAKKAR consortium (Barnier et al., 2007) with parameter settings as in Barnier et al. (2006) and Penduff et al. (2009).

2.2 Surface forcing

Surface atmospheric forcing for the period of 1989–2010 is obtained from ECMWF ERA-Interim 6 h reanalysis (Simmons et al., 2007; Dee and Uppala, 2009), which provides 10 m wind, 2 m air humidity and temperature for the bulk fluxes calculated from Large and Yeager (2004). Downwelling short- and long- wave radiative fluxes and precipitation over the oceans are daily averages, unmodified from ERA-Interim. Monthly climatological runoff (Dai and Trenberth, 2002) is applied along the land mask edge. This reanalysis also used a surface layer salinity relaxation/damping to climatological values, with a time scale of 180 days (36 days under ice).

2.3 Initial conditions and data assimilation

Initial conditions for temperature, salinity and circulation are derived from the end of a previous 1/4° reanalysis run from the same model in December 2004 (run UR025.1 described in Smith et al., 2009), which was forced with DFS3 meteorology (Brodeau et al., 2009). Most importantly, the initial conditions will have seen the start of the Argo profile assimilation and therefore will have more complete and consistent water properties from the beginning.

The data assimilation is restricted to temperature, T, and salinity, S, profile data, referred to as $S(T)$ (Haines et al., 2006; Smith and Haines, 2009), and is similar to what is currently employed in the ECMWF System 3 reanalysis (Balmaseda et al., 2008). It is a sequential scheme with optimal interpolation. Temperature profiles are assimilated along with a salinity balancing increment, as advocated by Troccoli and Haines (1999), and salinity profiles are then assimilated along isotherms (i.e. $S(T)$), up to latitudes of around 50° N/S. At higher latitudes salinity is assimilated in a univariate way on z-levels. Assimilation increments are calculated using a first guess at appropriate time (FGAT) every 5 days (73 cycles per year), and introduced evenly over the following day (known as incremental analysis updating; see Bloom et al., 1996). Observations are from the UK MetOffice quality-controlled ENACT/ENSEMBLES (EN3_v2a) data set (Ingleby and Huddleston, 2007), and they have not had any XBT bias corrections applied. This reanalysis run is referred to as UR025.3, and there is also a control run initialised and forced in the same way but without applying the data assimilation.

3 Heat fluxes, transports and budgets

The data assimilation method used is non-conservative and so heat, salt and freshwater content are changed by the assimilation increments and must be accounted for in any budget study (e.g. Fox and Haines, 2003; Zuo et al., 2011).

Figure 1a shows the mean sea surface temperature, SST, for the period 1993–2009, and Fig. 1b shows the differences from HadISST over the same period. Figure 1c shows the equivalent control run difference with HadISST. It can be seen that errors in the reanalysis are quite small everywhere, with much smaller biases throughout the tropics and in western boundary current regions than in the control run, or from previous runs of this model which used different meteorological forcings, e.g. Brodeau et al. (2009) (Fig. 12). This demonstrates that the data assimilation, although not directly assimilating SST, is sufficient to hold the surface properties much closer to observations. A full report on this reanalysis run can be found in Valdivieso and Haines (2011). These SST corrections have a significant influence on air-sea fluxes as will be seen later.

Figure 2 shows the time-evolving annual terms from the global ocean heat budget, including sea ice-covered areas, over the 17-year period. It can be seen that the dominant balance is between surface heat fluxes warming the oceans at a mean rate of Qnet$\sim$5.4 Wm^{-2}, balanced by data assimilation, integrated top-bottom, cooling the oceans at a mean rate of Qassim $\sim -4.9\,\mathrm{Wm}^{-2}$. The imbalance represents an average warming rate of 0.5 Wm^{-2}, which is captured accurately in the rate of increase in heat storage, Qt. This rate of increase in heat storage is quite consistent with estimates of the global radiation budget from the top of atmosphere measurements, e.g. Wong et al. (2009), showing that the total ocean state, including the deep ocean, is well aligned with observational data and is not drifting unrealistically.

The component of the excess surface heat flux balancing the data assimilation, i.e. 4.9 Wm^{-2}, can be regarded as predominantly an estimate of the global excess in downwelling shortwave radiation in the ERA-Interim product due to missing cloud effects, e.g. cloud opacity and regional biases such as in stratocumulus (Källberg, 2011; Dee et al., 2011). The assimilation compensates for this effect by removing excess heat. The directly estimated surface heat fluxes from the ERA-Interim atmospheric reanalysis, based on the specified surface SST, also have a net global downwelling radiation of $\sim$7 Wm^{-2} (Källberg, 2011). In the equivalent ocean

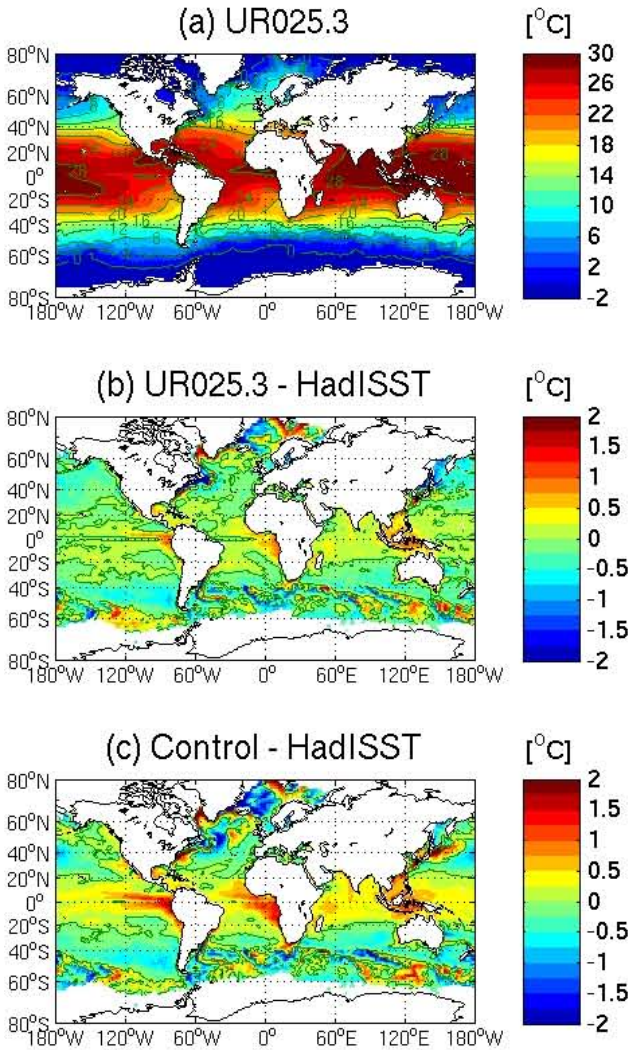

Fig. 1. (a) The mean sea surface temperature (SST) from the UR025.3 reanalysis for 1993–2009, **(b)** the difference between the mean SST and that from HadISST for the same period, **(c)** the difference between the equivalent model control run and HadISST through the same period.

control run without data assimilation, the model compensates by developing globally too high SSTs (Fig. 1c), allowing additional surface heat losses through sensible, and especially latent, heat fluxes, to compensate for the additional downwelling shortwave. The largest temporal anomaly in Fig 2 is the 1998 ENSO event when the ocean gain in heat storage peaks, followed by two years of net ocean heat loss. Assimilation clearly plays a significant role in this ENSO heat content cycle, although the net surface heat flux also shows a strong signal.

Table 1 gives the mean heat (and freshwater, FW) budgets globally and for each ocean basin, where the ocean basin boundaries are shown in Fig. 3. As with the heat budget, the sea ice is considered to be part of the ocean, so fluxes between water and ice do not need to be considered. The sea surface salinity relaxation is included as a contribution to the surface forcing. All advection terms were calculated from 5-day averages. In most basins the residuals are small compared to the 17-year storage changes and even in the Arctic and southern oceans, the budget residuals are much smaller than interannual storage signals. The Atlantic is gaining freshwater from the Arctic in the north and from the Southern Ocean in the south, and is thus a net evaporation basin, although this is only weakly indicated from the surface fluxes, with assimilation removing most of the FW. The Atlantic trend is to get warmer $\sim 2\,\mathrm{Wm}^{-2}$ and saltier (losing $9.6\,\mathrm{cm\,yr}^{-1}$ of FW). The Pacific gets warmer, also by $0.5\,\mathrm{Wm}^{-2}$, but fresher (gaining $1.8\,\mathrm{cm\,yr}^{-1}$ of FW), with the freshening attributable to the net precipitation, because the assimilation terms would make the basin saltier. The Indian Ocean also warms ($0.75\,\mathrm{Wm}^{-2}$) but with a very small trend in freshwater. The basin is seen to be a net evaporation basin with FW advected in and lost at the surface, again with assimilation playing a smaller role.

To investigate regional heat balances, we need to look at ocean heat transports. If we consider the 17-year heat budget as a function of latitude, Fig. 4a shows the global meridional ocean heat transports integrated southward from 90 N. The red line shows the actual heat transport calculated from 5 day model velocity, and temperature fields with the pink shading around it represent the interannual standard deviation in transport at each latitude. The solid blue line is the meridional heat transport based on the surface heat fluxes alone, assuming zero net storage of heat at all latitudes, and the dashed blue line shows the same calculation, with surface heat fluxes and data assimilation increments added together. Clearly, assimilation increments are needed to make the surface flux calculation consistent with the direct meridional transports (red curve), with the small discrepancies at the southern end resulting from the non-zero storage because the ocean is warming. Heat transports across a number of latitudes, based on the ocean section inverse models of Lumpkin and Speer (2007) and Ganachaud and Wunsch (2003), are also shown, with their estimated error bars. The global transport estimates are generally close to the ocean inverse estimates, except in the subtropics 24 N, which we see below is entirely due to the Atlantic.

The same transport calculations for the Atlantic Basin alone are shown in Fig. 4b. Although the peak northward transport in the Atlantic reaches 1.15 PW at 36 N, the transport is considerably reduced through most of the subtropics and generally below the inverse calculations from 20 S–30 N, although the error bars overlap with the interannual standard deviations from our model transports. The main reason for this is due to the lack of a bias correction for the assimilation increments at the Equator, where the sharp equatorial thermocline cannot be maintained properly, and assimilation increments then induce large secondary circulations (e.g. Bell et al., 2004). In a later reanalysis product, this effect has been

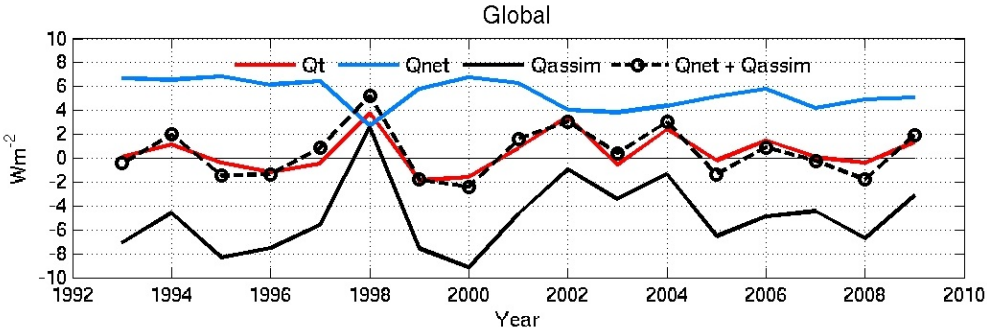

Fig. 2. Annual time series of the global ocean heat budget from 1993–2009. The terms are Qnet, the surface heat flux; Qassim, the equivalent heat flux coming from data assimilation increments vertically integrated; and Qt, the heat storage associated with changes in global mean temperature.

Table 1. Vertically integrated heat and freshwater budget averaged over the period 1990–2009 for the global ocean and for individual oceanic basins (domains shown in Fig. 3). Upper numbers indicate heat fluxes in Wm^{-2}; lower numbers indicate freshwater fluxes in $cm\,yr^{-1}$ and errors represent annual standard deviations. The residual is computed as the sum of advection, surface forcing and assimilation minus the contribution from the storage. Positive values indicate fluxes into the ocean.

Basin Areas m^2	Advection	Surface Forcing	Assimilation	Storage	Residual
Global	0.00 ± 0.00	5.39 ± 1.23	-4.90 ± 3.01	0.48 ± 1.62	0.01 ± 0.89
(3.61e+14)	-0.01 ± 0.00	4.00 ± 1.99	-5.46 ± 9.61	-1.62 ± 8.81	0.15 ± 1.91
Atlantic	3.06 ± 1.01	7.53 ± 1.96	-9.34 ± 7.14	2.18 ± 6.46	-0.93 ± 1.87
(6.87e+13)	22.20 ± 4.03	-10.49 ± 2.40	-23.79 ± 36.92	-9.65 ± 35.97	-2.42 ± 4.39
Pacific	-7.28 ± 0.97	14.36 ± 2.50	-6.75 ± 3.80	0.50 ± 3.66	-0.17 ± 1.07
(1.35e+14)	0.88 ± 1.12	3.38 ± 3.91	-3.05 ± 8.39	1.79 ± 8.30	-0.58 ± 1.64
Indian	-5.01 ± 2.55	10.83 ± 2.82	-5.22 ± 4.28	0.75 ± 5.92	-0.16 ± 1.30
(4.31e+13)	30.15 ± 4.27	-20.48 ± 3.67	-11.86 ± 17.24	-0.58 ± 16.83	-1.61 ± 3.06
South. Ocean	7.71 ± 1.23	-7.03 ± 1.31	-0.50 ± 6.90	-0.88 ± 5.92	1.06 ± 2.25
(1.02e+14)	-25.30 ± 2.69	18.34 ± 1.85	7.73 ± 14.40	-1.74 ± 13.04	2.50 ± 6.24
Arctic	16.40 ± 1.60	-21.05 ± 1.91	4.72 ± 4.23	1.00 ± 3.51	-0.94 ± 0.80
(1.23e+13)	-29.37 ± 7.37	57.30 ± 12.12	-16.16 ± 31.48	2.87 ± 28.25	8.90 ± 7.37

greatly reduced. At higher latitudes in the Atlantic, however, the transports in this reanalysis agree very well with inverse estimates, e.g. at 30 S or 47 N. In Sect. 5 we will look in more detail at the transports at 26 N in the Atlantic, where the RAPID transport array (Cunningham et al., 2007), now provides independent evaluation measurements.

Figure 5 shows the mean Southern Ocean heat transports across several sections. The model transports are generally in very good agreement for all the sections, especially over the last period constrained well by Argo (2005–2009). Again, the interannual standard deviation in transports is shown, along with the transport trends. There are no statistically significant trends seen in any of these transports.

On the global scale, the dominant balance in the heat budget is between surface fluxes adding heat, and data assimilation removing heat. At the local scale, particularly near strong currents, the balance is generally three ways between surface fluxes, data assimilation and the mean heat transport convergence, with the last two usually showing larger spatial variability, as previously found in other data assimilation experiments (e.g. Haines 2003, Fig. 6). Here in Fig. 6 we show, for example, details of these three terms in the heat budget over the subpolar gyre of the North Atlantic, along with an independent estimate of the surface fluxes from OAFlux (Yu et al., 2008). The resolved surface heat fluxes reproduce the spatial distribution of the OAFlux product rather well, with a very similar position for the reversal from warming to cooling across the Atlantic Basin. The dipole in transport convergence along the Gulf Stream path, suggesting a tendency for the Gulf Stream to drift north, is balanced by data assimilation, tending to move the current and heat content back to a more correct southerly position. Around the subpolar gyre, transport convergence of heat around the boundary and along steep topography, e.g. the edge of the Labrador Sea and also the Reykjanes Ridge, is removed by the data assimilation increments. The assimilation at these scales appears to be compensating for the lack of eddy heat transport, because it is taking heat away from the boundary currents and depositing it

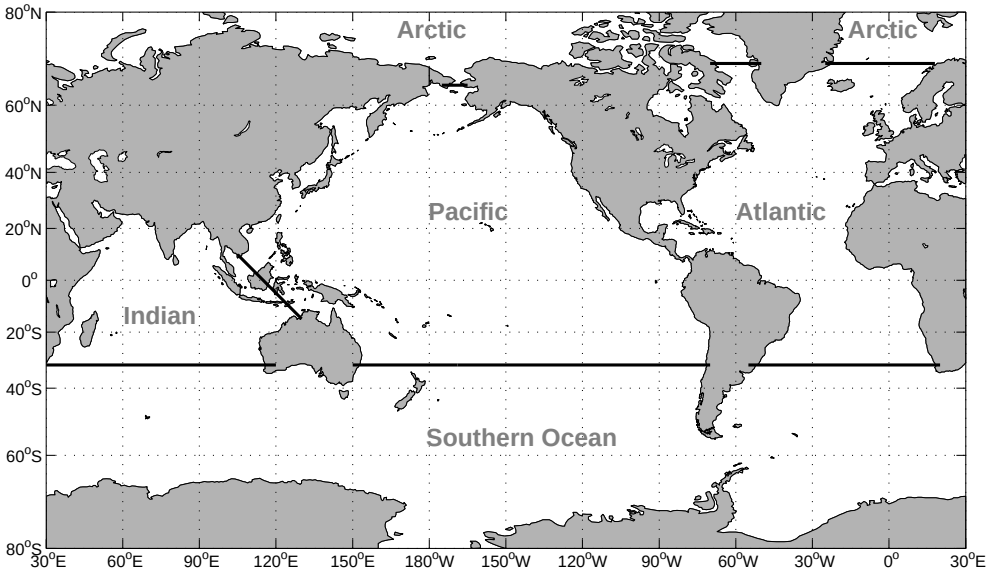

Fig. 3. Domains of the different ocean basins used for calculating the heat and freshwater budgets shown in Table 1. In the Southern Ocean to division is at 32 S. In the North Atlantic the separation with the Arctic Basin is at approximately 70 N, but following the ORCA model grid.

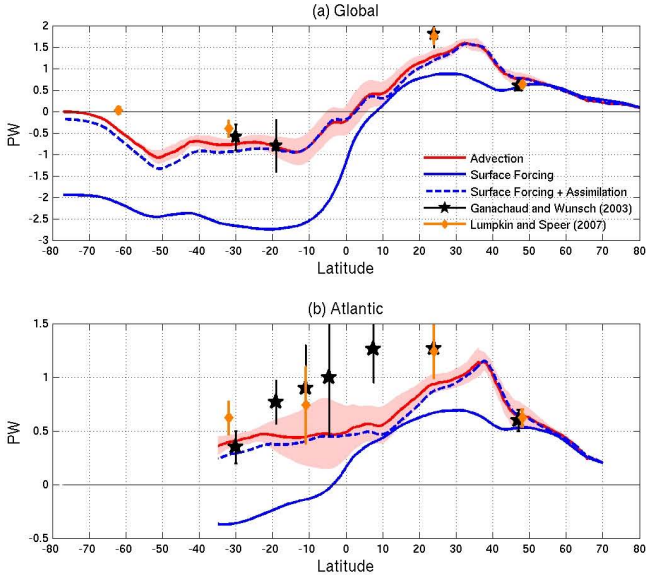

Fig. 4. Meridional heat transports from UR025.3 over 1993–2009 for **(a)** the global ocean and **(b)** the Atlantic Basin. The Advection (red) is based on the resolved velocity and temperatures fields, including all eddy components down to the 5 day time scale. The shaded area shows the annual standard deviations in advective transport. The solid blue line uses surface heat fluxes and a steady state assumption to calculate meridional heat transport, and the dashed blue line uses surface heat fluxes combined with assimilation increments to do the same.

in the basin interior, which is exactly the role that baroclinic eddies would be expected to play. Despite the relatively high model resolution, eddy transports are clearly insufficient at these latitudes in the subpolar gyre.

4 Freshwater fluxes, transports and budgets

We have also assessed the mean model freshwater fluxes and transports against independent observational estimates. The surface fluxes of freshwater are complicated by the existence of the surface salinity relaxation term, which has often been used in model simulations, because the surface salinity is not closely coupled to atmospheric conditions and so is free to drift. In a new reanalysis for MyOcean v2, we have removed this term altogether, instead relying on data assimilation to counter any surface salinity drift tendency.

Figure 7 shows the time-evolving annual terms from the global freshwater budget over the 17-year period. As in the global heat budget (Fig. 2), the dominant balance in the freshwater budget is between a surface gain in freshwater, Fnet, at a mean rate of 4.0 cm yr^{-1} (including surface relaxation), balanced by assimilation loss of freshwater, Fassim, at $\sim$5.5 cm yr^{-1}. The interannual variability of the assimilation term is very large, however, particularly prior to and during the period when the Argo array gets up and running between 1999–2004, as much of the ocean starts to have salinity observations down to 2000 m for the first time. After 2004 the freshwater budgets show signs of being much more in balance again from year to year, as the Argo array becomes established.

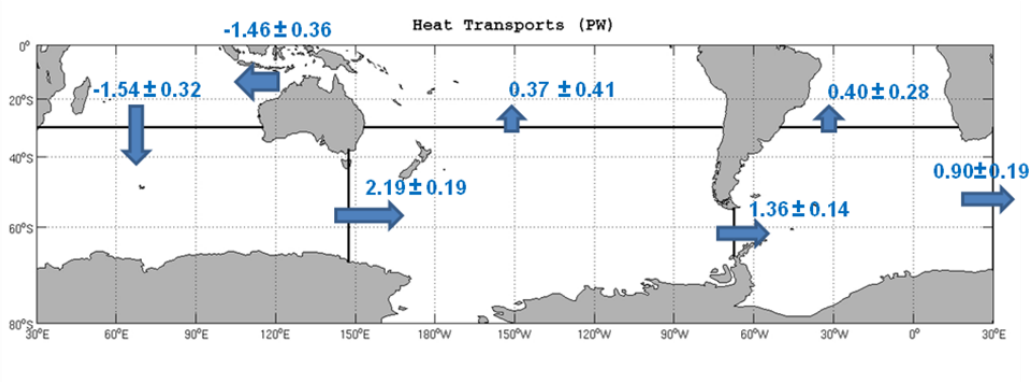

Section	UR025.3 1993 – 2009 Mean + STD	UR025.3 2005 – 2009 Mean + STD	UR025.3 1993 – 2009 Linear Trend	Inverse Analysis Mean + STD
Drake Passage	1.35 ± 0.13	**1.36 ± 0.14**	-0.0017	1.36 ± 0.09
South A. – Antarctica 30° E	0.95 ± 0.20	**0.90 ± 0.19**	-0.0020	0.88 ± 0.24
Australia – Antarctica 143° E	2.20 ± 0.19	**2.19 ± 0.19**	-0.0013	1.85 ± 0.18
Indonesian Throughflow	-1.35 ± 0.37	**-1.46 ± 0.36**	-0.0107	-1.46 ± 0.21
Indian 32° S	-1.50 ± 0.29	**-1.54 ± 0.32**	-0.0039	-1.55 ± 0.12
Pacific 32° S	0.34 ± 0.44	**0.37 ± 0.41**	+0.0080	0.55 ± 0.15
Atlantic 32° S	0.40 ± 0.22	**0.40 ± 0.28**	+0.0016	0.62 ± 0.15

Fig. 5. Heat transports and their annual standard deviations, in PW, through major sections in the Southern Hemisphere in UR025.3 over the periods 1993–2009 and through 2005–2009, in comparison to estimates from the inverse model results of Lumpkin and Speer (2007).

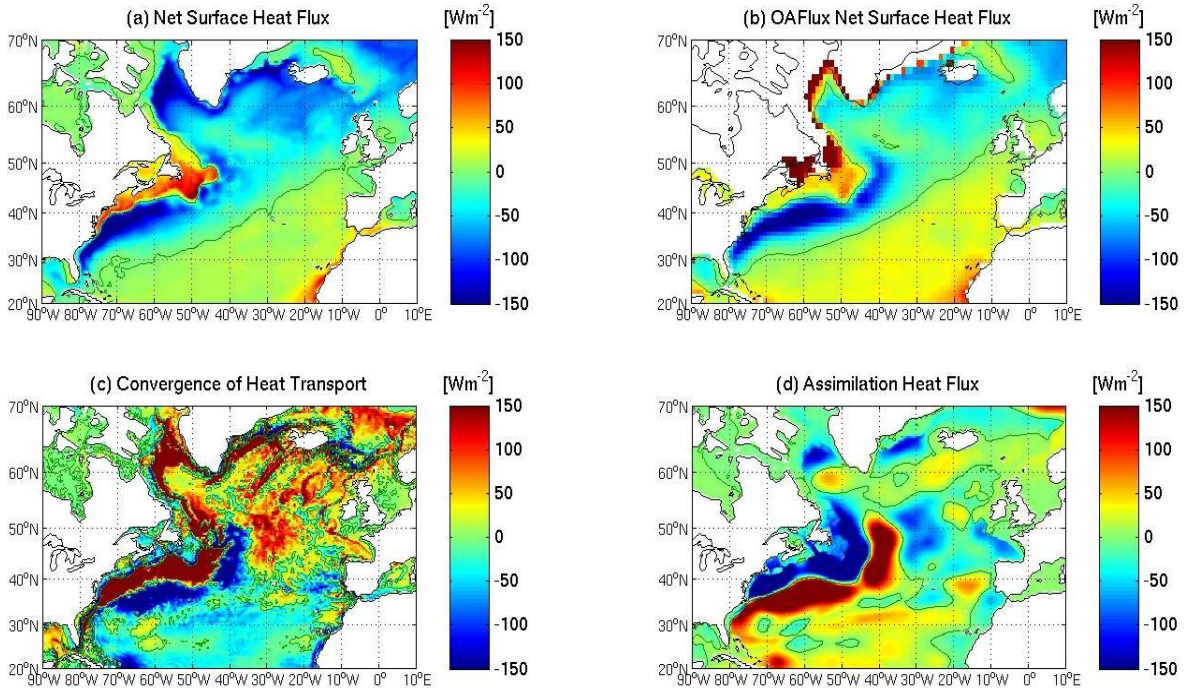

Fig. 6. Main components of the heat budget over the North Atlantic in UR025.3 for 1993–2009. **(a)** Net surface heat flux, **(c)** Heat transport convergence, **(d)** Assimilation increments equivalent heat flux. **(b)** provides a comparison from an independent surface heat flux product OAFlux (from Wong et al., 2009).

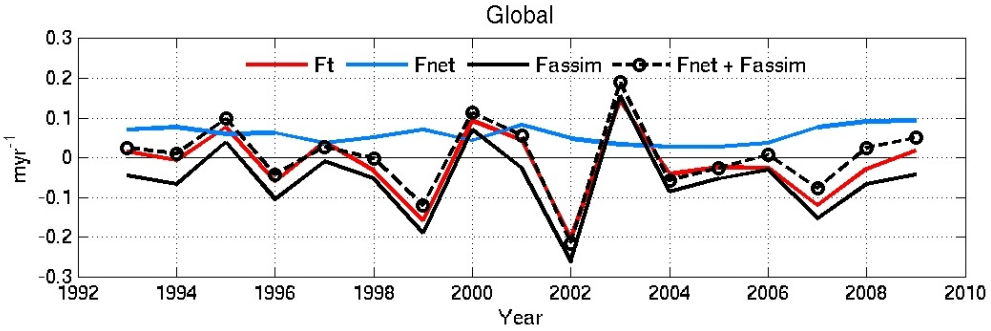

Fig. 7. Annual time series of the global ocean freshwater budget from 1993–2009. The terms are Fnet, the surface freshwater flux; Fassim, the equivalent freshwater flux coming from data assimilation increments vertically integrated; and Ft, the freshwater storage associated with changes in global mean salinity.

From the Fnet and Fassim values above, one might think this implies a global sea level fall of 1.5 cm yr^{-1}, but the damping and the salinity data assimilation use virtual salt fluxes rather than freshwater fluxes. The sea surface salinity damping contributes a surface loss of freshwater at a mean rate ∼2 cm yr^{-1}, so the actual imbalance to the addition of water leads to a net sea level rise in the model at a rate of ∼6 cm yr^{-1}, although the total effect on the storage from the virtual salt flux terms means the ocean gets saltier over the period.

If we assume that the ocean should have an approximately closed water budget over the period (neglecting any real sea level change terms ∼mm yr^{-1}), then we can take the data assimilation and surface salinity damping terms together, minus the change in storage, as giving an estimate of the excess precipitation in the ERA-Interim product (assuming that evaporation is now calculated correctly from the bulk formulae based on the assimilation corrected SST fields in Fig. 1a), implying a precipitation excess of ∼6 cm yr^{-1} over the oceans. Kållberg (2011) and Dee et al. (2011) also comment on the excess in net precipitation in the ERA-Interim products, which vary with time. Alternatively, the additional latent heat required to evaporate ∼6 cm yr^{-1} of excess precipitation turns out to be ∼4.7 Wm^{-2}, which is very close to the excess surface heating removed by data assimilation in the global heat budget. Indeed in the control run without data assimilation, the model achieves both a balanced heat and freshwater budget just through having the higher SSTs (in Fig. 1c), which lead to higher surface heat loss and freshwater loss through evaporation of an extra 6–7 cm yr^{-1} of water from the ocean surface.

We can see how the freshwater budget is balanced as a function of latitude in Fig. 8a which shows zonal-averaged results for the global ocean, and Fig. 8b for the Atlantic only. The red line shows the freshwater (FW) transport across each latitude circle south from 90 N in Fig. 8a, and from 66 N in Fig. 8b (the latitude of the Bering Straits), calculated directly from the model velocity fields and using a salinity reference value equivalent to each section average salinity. The pink shaded area around this line shows the standard deviation of annual variability in transports about the 17-year mean. The blue line shows the FW transports calculated from the surface fluxes (E-P-R) alone, integrated southward while assuming no FW storage, as in Wijfells (2001). The blue dashed line is the same as the blue line, but including the surface salinity damping and the data assimilation terms, which clearly bring the results into close agreement with the direct FW transport assessments. The values in the Atlantic at 66 N are made to agree to avoid some of the problems associated with Bering Strait transports and Arctic ice fluxes which occur further north.

Meridional ocean freshwater transports as in Fig. 8a and b can be evaluated in two ways: against individual ocean hydrographic sections, or against inverse models, using specific latitudes, some of which are marked on Fig. 8a and b. Also, the ocean FW transports can be matched against atmospheric FW transports calculated from atmospheric reanalysis products, or against independent surface FW flux estimates, many results of which can be found in Wijffels (2001) (Fig. 6.2.6–6.2.9). The estimates from this ocean reanalysis are broadly consistent with these previous estimates, and the interannual standard deviation gives some idea of the error incurred by inverse models when using single section data taken in one particular year to estimate transports.

5 Role of the Atlantic MOC

The meridional overturning circulation in the Atlantic plays a key role in controlling both meridional heat and freshwater transports and influencing North Atlantic SSTs (e.g. Knight et al., 2005; Delworth et al., 2007; Robson et al., 2012). At 26.5 N the time series of the meridional heat transport is now continuously monitored by the RAPID array program (Cunningham et al., 2007). Figure 9 shows the monthly and annual time series of Atlantic MOC at 26 N from our reanalysis from 1989–2010, along with the MOC derived from the RAPID array from 2004 onwards. Since much of the variability is the direct result of wind stress, the correspondence with the observational variability in the RAPID array period in both

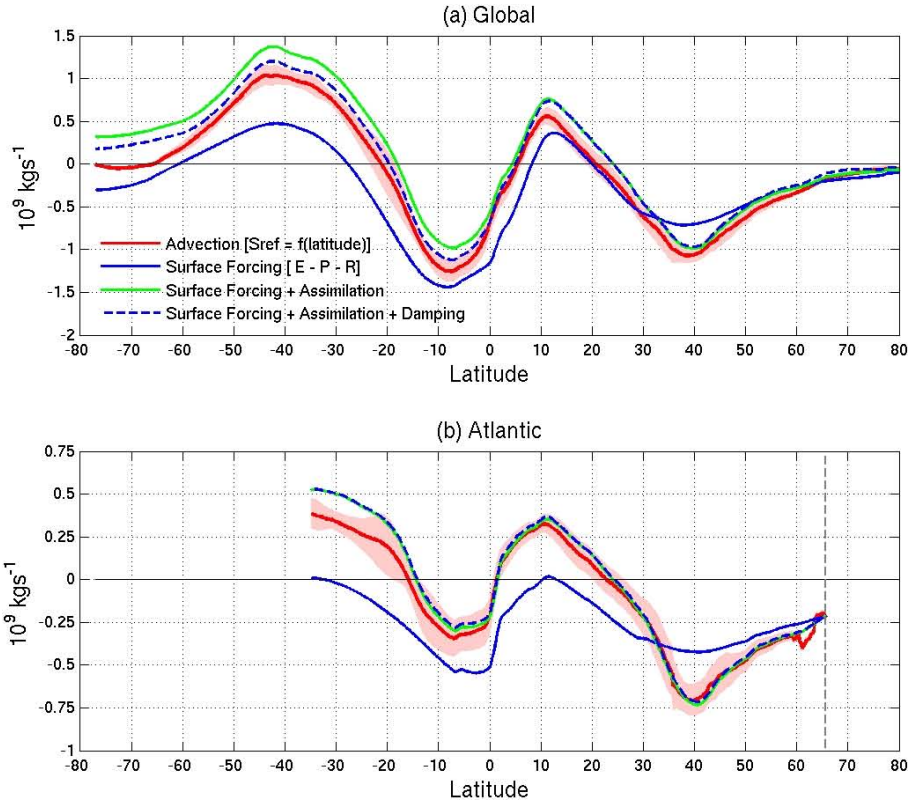

Fig. 8. Meridional freshwater transports from UR025.3 over 1993–2009 for **(a)** the global ocean and **(b)** the Atlantic Basin. The Advection (red) is based on the resolved velocity and salinity fields, including all eddy components down to the 5 day time scale. The shaded area shows the annual standard deviations in advective transport. The solid blue line uses surface freshwater fluxes and a steady state assumption to calculate meridional freshwater transport, and the dashed blue line uses surface freshwater fluxes combined with assimilation increments to do the same.

figures is clear. The mean MOC for the long period 1993–2009 is 17.0 Sv and during the RAPID array period 2004–2009, it is 17.3 Sv compared with the RAPID observational value of 17.5 Sv for this period. It is interesting to note that the model annual mean values in 1992 and 1998, indicating a decline over the period, compare very well to the Bryden et al. (2005) section estimates also shown in the figure. Between 1990 and 2000, the MOC in fact shows a peak around 1994–1995, which is now also consistent with other reanalysis estimates e.g. Pohlmann et al. (2011), which is probably driven by variations in the NAO and associated buoyancy forcing, e.g. Robson et al. (2012).

Turning to the heat transports at 26 N in the Atlantic, from Fig. 4b there is a low northward transport of ∼1.09 PW compared to observations of ∼1.3 PW, with virtually the same low discrepancy showing up in the global values. However, the model's 1993–2009 mean meridional overturning circulation at 26 N is 17.0S v, which is close to recently observed estimates based on RAPID array data at 18.5 Sv (Cunningham et al., 2007), so why is the heat transport anomalously lower? Johns et al. (2011) estimated the 26 N Atlantic heat transport and its components from the RAPID boundary array from April 2004–October 2007 inclusive, and we show these values along with the equivalent from our model in Table 2 below.

The total mean heat transport of 1.09 PW is considerably lower than the 1.35 PW estimated by Johns et al. (2011), and it is important to understand the origin of these differences. The Florida Strait component of the MOC with a mean transport of 32.6 Sv and a heat transport of 2.55 PW is remarkably close to observations, particularly given that the control run has a much lower Florida Strait transport. The potential of assimilation to increase the Florida Strait current was previously noted by Smith et al. (2010) and by Stepanov et al. (2012). The mean Ekman transport at 3.2 Sv is lower than used by Johns et al. (2011) of 3.5 Sv, leading to a lower heat transport of 0.28PW compared with 0.35 PW. This is the result of the QuickScat wind products used by Johns et al. (2011) being stronger than ERA-Interim. The main discrepancy however comes from the zonal mean mid-ocean transport which, at –1.82 PW, is significantly stronger than the observed mid-ocean transport of –1.64 PW (including the WB-Abaco flows close to the Bahamas). These two terms explain the main differences between model and observations, with the zonally varying eddy component of the heat transport at 0.08PW being very similar again to observations. If

Table 2. Decomposition of the Atlantic 26 N meridional heat transport in UR025.3 over the 3.5-year period Apr 2004–Oct 2007, compared with Johns et al. (2011) RAPID estimates for the same period, along with the meridional overturning components. Note that the UR025.4 Mid-ocean heat transport includes all transport east of the Bahamas, including Abaco. Corresponding standard deviations are given in round brackets. For the full 2004–2010 period, the RAPID MOC is 18.6 (3.7) Sv and UR025.3 MOC is 17.3 (3.3) Sv.

Meridional heat transport component	RAPID mean (std), PW	UR025.3 mean(std), PW	Transport in RAPID mean (std) Sv **(MOC = 16.6 (2.6))**	Transport in UR025.3 mean (std) Sv **(MOC = 17.6 (3.5))**
Florida Current	2.53 (0.24)	2.55 (0.23)	31.7 (2.8)	32.6 (2.4)
Ekman	0.35 (0.34)	0.28 (0.18)	3.5 (2.3)	3.2 (1.7)
Mid-ocean	–1.77 (0.25)	–1.82 (0.23)	–36.5 (4.4)	–37.4 (2.9)
WB-Abaco	0.13 (0.16)	–	1.3 (–)	
Eddy	0.11 (0.04)	0.08 (0.03)	–	
Total	1.35 (0.40)	1.09 (0.27)	0.0	–1.6

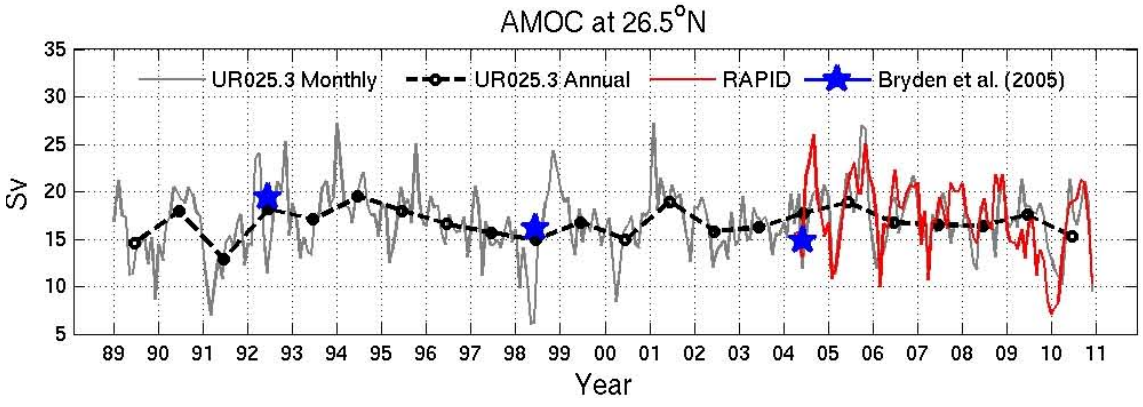

Fig. 9. Monthly and annual mean time series of the Atlantic meridional overturning circulation (AMOC), from UR025.3 in comparison with the RAPID array values from 2004–2010. Also shown are the mean section-based estimates in 1992, 1998 and 2004 (from Bryden et al., 2005). Bryden et al use an annual mean Ekman component in an attempt to represent annual mean values at these sections.

we use the temperature cross section of Johns et al. (2011) along with our modelled velocity fields, the heat transports are Ekman = 0.29 PW and mid-ocean transport = –1.76 PW, showing that the heat transport differences come mainly from the current distributions rather than temperature differences.

Recently, there has also been much interest in the role of the meridional overturning circulation in transporting freshwater in the Atlantic. In Fig. 10 we therefore separate the total meridional FW transport in the Atlantic (shown in Fig. 8b) into the component of freshwater transported by the vertical overturning circulation, also called the Mov (e.g. Drijfhort et al., 2011). The vertical overturning transport component is calculated from the zonal- averaged baroclinic currents and the zonal average salinity. The gyre transport is approximately given by the difference between the two curves shown. It can be seen that at around 30 S the overturning component of freshwater transport is negative, i.e. southwards out of the Atlantic, despite the fact that the total ocean freshwater transport is northward into the Atlantic Basin. This southward overturning transport at 30 S has been suggested as an indicator of instability in the Atlantic overturning circulation (e.g. Dijkstra, 2007; Hawkins et al., 2011), because a decrease in the overturning circulation would then tend to make the Atlantic Basin fresher, perhaps reducing the high latitude water formation that drives the overturning. The reanalysis confirms the sign of overturning freshwater transport at 30 S found in other observationally-based analyses, and shows that this transport component remains negative through nearly the whole Atlantic Basin. However, the argument for the overturning freshwater transport at 30 S, determining the stability of the Atlantic overturning, assumes that variations in other components of the meridional freshwater budget between 30 S and the deep water formation latitudes in the North Atlantic, e.g. the gyre FW transport or the surface evaporation (as determined by SST), would not be temporally correlated with the overturning transport changes. This aspect of the Atlantic freshwater transports will be investigated in greater detail in a future study.

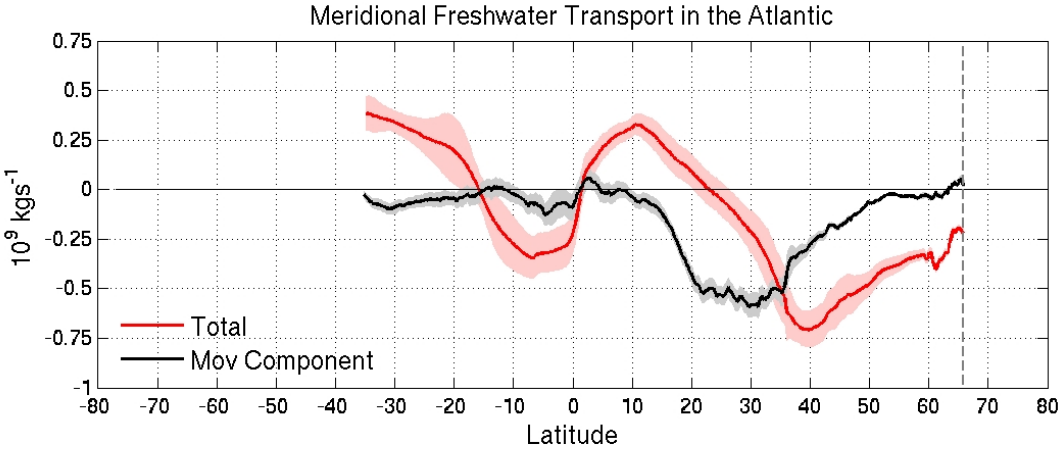

Fig. 10. The time mean meridional freshwater transport in the Atlantic at all latitudes, from UR025.3. The total meridional transport and the "MOV" component, due to the vertical overturning alone, are both shown. The shaded areas are the annual standard deviations.

6 Summary and conclusions

In this paper we have looked at the reproduction of heat and freshwater budgets and transports in a 1/4° global ocean reanalysis product prepared as part of the EU GMES Marine Service. The intention was to show that the budgets of heat and freshwater can be consistently explained, despite the presence of "unphysical" data assimilation terms. Second, the data assimilation terms can be interpreted as making corrections to the resolved physical processes acting in the model and third, the horizontal transports in the model are mostly very well reproduced compared with independent observation-based estimates, and these transports do not show unphysical trends that are common in ocean model simulation runs.

On the global scale the data assimilation increments are shown to counteract global imbalances in surface forcing, in particular correcting for higher incidence of solar shortwave radiation (Kållberg, 2011; Dee et al., 2011) by removing heat, and also correcting for a higher-than-average global precipitation in ERA-Interim (Kållberg, 2011) by adding salt. For the zonally-integrated meridional transport budgets, the inclusion of the data assimilation terms effectively closes the budgets at all latitudes, showing that the assimilating model only exhibits small trends that are consistent with real upper ocean changes.

At regional scales the interpretation of the assimilation increments in the regional budgets relies on knowing and trusting the heat and freshwater flux divergences. This is the same assumption that is commonly made when atmospheric reanalyses are used to assess surface fluxes and regional budgets of heat and freshwater (e.g. as in Trenberth et al., 2011). Thus, the approach being followed here is following the atmospheric methodology but applying it to ocean reanalyses. In order to do this we must rely on reproducing good ocean transports through strong constraints on the geostrophic flows.

The modelled transports assessed against trans-oceanic section-based estimates are shown to be very realistic, e.g. throughout the southern oceans and within the Pacific and Indian Basins. Zuo et al. (2011) have previously shown that the transports into/out of Arctic latitudes in this reanalysis are also reasonably consistent with observations. There are some discrepancies in meridional heat transport across the Equator in the Atlantic and up as far as the subtropical gyre. The transports at 26 N are compared in detail with the RAPID array estimates of Johns et al. (2011), and it is shown that discrepancies mainly lie in the mid-ocean component of the heat transport, although the Ekman transport is also slightly lower, based on using weaker surface winds in ERA-Interim compared with QuickScat.

The meridional freshwater transports in the model compare reasonably well with previous estimates, although there is a much higher degree of uncertainly because of the greater scarcity of accurate salinity measurements in the ocean prior to Argo, and due to the independent difficulties of estimating precipitation over the oceans. The meridional transport of freshwater by the overturning circulation has been estimated at all latitudes in the Atlantic and shown to be highly variable, although the southward freshwater transport around 30 S in the Atlantic appears to be a robust result throughout the 17-year reanalysis period.

A new reanalysis is currently underway using a more comprehensive data assimilation system, including altimeter, sea surface temperature and sea ice concentration increments, in addition to the ocean profile assimilation used here, based on the full FOAM data assimilation system currently in operational oceanography use at the UK Met Office. Other reanalyses from the EU MyOcean program will also be available in a uniform format that will allow similar diagnostic comparisons. In a future study we will use a similar suite of diagnostics to assess the robustness of these results between models and assimilation systems. It is only through

such robust comparisons can we begin to learn to interpret data assimilation results more quantitatively and begin an effective investigation of model error processes.

Acknowledgements. This work was supported by grants from NERC through the National Centre for Earth Observation, the Rapid-Watch Valor project, and from the EU GMES MyOcean project. The authors also thank ECMWF for special project spgbdaoc computer resources, without which this work would not have been possible.

Edited by: P.-Y. Le Traon

References

Adcroft A., Hill C., and Marshall, J.: Representation of topography by shaved cells in a height coordinate ocean model, Mon. Wea. Rev., 125, 2293–2315, 1997.

Balmaseda, M. A., Vidard, A., and Anderson, D. L. T.: The ECMWF ORA-S3 ocean analysis system, Mon. Wea. Rev., 136, 3018–3034, 2008a.

Barnier, B. and the DRAKKAR Group: Eddy-permitting ocean circulation hindcasts of past decades, Clivar Exchanges, 12, 8–10, 2007.

Barnier, B., Madec, G., Penduff, T., Molines, J. M., Treguier, A. M., Le Sommer, J., Beckmann, A., Biastoch, A., Böning, C., Dengg, J., Derval, J., Durand, E., Gulev, S., Remy, E., Talandier, C., Theetten, S., Maltrud, M., McClean, J., and De Cuevas, B.: Impact of partial steps and momentum advection schemes in a global ocean circulation model at eddy-permitting resolution, Ocean Dynam., 56, 6543–567, doi:10.1007/s10236-006-0082, 2006.

Bell, M. J., Martin, M. J., and Nichols, N. K.: Assimilation of data into an ocean model with systematic errors near the Equator, Q. J. Roy. Meteor. Soc., 130, 873–893, 2004.

Bloom, S., Takacs, L., DaSilva, A., and Ledvina, D.: Data assimilation using incremental analysis updates, Mon. Wea. Rev., 124, 1256–1271, 1996.

Boyer, T. P., Garcia, H. E., Johnson, D. R., Locarnini, R. A., Mishonov, A. V., Pitcher, M. T., Baranova, O. K., and Smolyar, I. V.: World Ocean Database 2005, NOAA Atlas NESDIS 60, edited by: Levitus, S., 190 pp. U.S. Gov. Print. Off.: Washington D. C., 2006.

Brodeau, L., Barnier, B., Treguier, A. M., Penduff, T., and Gulev, S.: An ERA40-based atmospheric forcing for global ocean circulation models, Ocean Modell., 31, 88–104, doi:10.1016/j.ocemod.2009.10.005, 2009.

Bryden, H. L., Longworth, H. L., and Cunningham, S. A.: Slowing of the Atlantic Meridional Overturning Circulation at 25° N, Nature, 438, 655–657, 2005.

Carton, J. A. and Giese, B. S.: A reanalysis of ocean climate using Simple Ocean Data Assimilation (SODA), Mon. Wea. Rev., 136, 2999–3017, 2008.

Cunningham, S. A., Kanzow, T., Rayner, D., Baringer, M. O., Johns, W. E., Marotzke, J., Longworth, H. R., Grant, E. M., Hirschi, J. J.-M., Beal, L. M., Meinen, C. S., and Bryden, H. L.: Temporal Variability of the Atlantic Meridional Overturning Circulation at 26.5° N, Science, 317, 935–938, 2007.

Dai, A. and Trenberth, K. E.: Estimates of freshwater discharge from continents: Latitudinal and seasonal variations, J. Hydrometeorol., 3, 660–687, 2002.

Dee, D. P. and Uppala, S.: Variational bias correction of satellite radiance data in the ERA-Interim reanalysis, Q. J. Roy. Meteor. Soc., 135, 1830–1841, 2009.

Dee, D. P., Uppala, S. M., Simmons, A. J., Berrisford, P., Poli, P., Kobayashi, S., Andrae, U., Balmaseda, M. A., Balsamo, G., Bauer, P., Bechtold, P., Beljaars, A. C. M., van de Berg, L., Bidlot, J., Bormann, N., Delsol, C., Dragani, R., Fuentes, M., Geer, A. J., Haimberger, L., Healy, S. B., Hersbach, H., H'olm, E. V., Isaksen, L., Krallberg, P., Köhler, M., Matricardi, M., McNally, A. P., Monge-Sanz, B. M., Morcrette, J.-J., Park, B.-K., Peubey, C., de Rosnay, P., Tavolato, C., Th'epaut, J.-N., and Vitart, F.: The ERA-Interim reanalysis: configuration and performance of the data assimilation system. Q. J. Roy. Meteor. Soc., 137, 553–597, doi:10.1002/qj.828, 2011.

Delworth, T. L., Zhang, R., and Mann, M. E.: Decadal to centennial variability of the Atlantic from observations and models In Ocean Circulation: Mechanisms and Impacts, Geophysical Monograph Series 173, Washington, DC, Am. Geophys. Union, 131–148, 2007.

Döscher, R., Böning, C., and Herrmann, P.: Response of circulation and heat transport in the north Atlantic to changes in thermohaline forcing in northern latitudes: A model study, J. Phys. Oceanogr., 24, 2306–2320, doi:10.1175/1520-0485(1994)024, 1994.

DRAKKAR Group, 2007: Eddy-permitting Ocean Circulation Hindcasts of past decades, CLIVAR Exchanges No 42, 12(3), 8-10, edited by: Drijfhout, S. S., Weber, S. L., and van der Swaluw, E., The stability of the MOC as diagnosed from model projections for pre-industrial, present and future climates, Clim. Dyn., 2011, 37, 7–8, 1575–1586, doi:10.1007/s00382-010-0930-z, 2011.

Dijkstra, H. A.: Characterization of the multiple equilibria regime in a global ocean model, Tellus A, 59, 695–705, doi:10.1111/j.1600-0870.2007.00267.x, 2007.

Fichefet, T. and Maqueda, M.: Sensitivity of a global sea ice model to the treatment of ice thermodynamics and dynamics, J. Geophys. Res., 102, 12609–12646, 1997.

Fox, A. D and Haines, K.: Interpretation of Water transformations diagnosed from data assimilation, J. Phys. Oceanogr., 33, 485–498, 2003.

Ganachaud, A. and Wunsch, C.: Large scale ocean heat and freshwater transports during the World Ocean Circulation Experiment, J. Climate., 16, 696–705, 2003.

Goose, H. and Fichefet, T.: Importance of ice-ocean interactions for the global ocean circulation: A model study, J. Geophys. Res., 104, 23337–23355, 1999.

Grist, J. P., Josey, S. A., Marsh, R., Good, S. A., Coward, A. C., de Cuevas, B. A., Alderson, S. G., New, A. L., and Madec, G.: The Roles of surface heat flux and ocean heat transport convergence in determining Atlantic Ocean temperature variability, Clim. Dynam., 60, 771–790, doi:10.1007/s10236-010-0292-4, 2010.

Haines, K.: Ocean Data Assimilation, NATO ISI Series Maratea Italy 289–320, 2003.

Haines, K., Blower, J., Drecourt, J.-P., Liu, C., Vidard, A., Astin, I., and Zhou, X.: Salinity assimilation using S(T): Covariance relationships, Mon. Weath. Rev., 134, 759–771, 2006.

Häkkinen, S. and Rhines, P.: Decline of Subpolar North Atlantic Circulation During the 1990s, Science, 304, 555–559, doi:10.1126/science.1094917, 2004.

Hawkins, E., Smith, R. S., Allison, L. C., Gregory, J. M., Woollings, T. J., Pohlmann, H., and de Cuevas, B.: Bistability of the Atlantic overturning circulation in a global climate model and links to ocean freshwater transport, Geophys. Res. Lett., 38, L10605, doi:10.1029/2011GL047208, 2011.

Ingleby, B. and Huddleston, M.: Quality control of ocean temperature and salinity profiles – historical and real-time data, J. Mar. Sys., 65, 158–175, 10.1016/j.jmarsys.2005.11.019, 2007.

Johns, W. E., Baringer, M. O., Beal, L. M., Cunningham, S. A., Kanzow, T., Bryden, H. L., Hirschi, J. J. M., Marotzke, J., Meinen, C. S., Shaw, B., and Curry, R.: Continuous, Array-Based Estimates of Atlantic Ocean Heat Transport at 26.5° N, J. Climate, May 2011, 24, 2429–2449, doi:10.1175/2010JCLI3997.1, 2011.

Kållberg, P.: Forecast drift in ERA-Interim, ERA Report Series, No. 10, ECMWF: Reading, UK, http://www.ecmwf.int/publications/library/ecpublications/_pdf/era/era_report_series/RS_10.pdf 2011.

Knight, J. R., Allan, R. J., Folland, C. K., Vellinga, M., and Mann, M. E.: A signature of persistent natural thermohaline circulation cycles in observed climate, Geophys. Res. Lett., 32, L20708, doi:10.1029/2005GL024233, 2005.

Large, W. G. and Yeager, S. G.: Diurnal to decadal global forcing for ocean and sea-ice models: The data sets and flux climatologies, Technical Report TN-460+STR, NCAR, 105 pp., 2004.

Lazier, J., Hendry, R., Clarke, A., Yashayaev, I., and Rhines, P.: Convection and restratification in the Labrador Sea, 1990–2000, Deep-Sea Res. Pt. I, 49, 1819–1835, 2002.

Levitus, S., Antonov, J. I., Boyer, T. P., and Stephens, C.: Warming of the World Ocean, Science, 287, 2225–2229, doi:10.1126/science.287.5461.2225, 1998.

Lumpkin, R. and Speer, K.: Global Ocean Meridional Overturning, J. Phys. Oceanogr., 37, 2550–2562, doi:10.1175/JPO3130.1, 2007.

Madec, G., Delecluse, P., Imbard, M., and Levy, C.: OPA 8.1 general circulation model reference manual. Notes de l'IPSL, University P. et M. Curie, B102 T15-E5, Paris, No. 11, 91, 1998.

Madec, G.: NEMO reference manual, ocean dynamics component : NEMO-OPA. Preliminary version. Note du Pole de modélisation, Institut Pierre-Simon Laplace (IPSL), France, No. 27 ISSN No 1288–161, 2008.

Penduff, T., Le Sommer, J., Barnier, B., Treguier, A.-M., Molines, J.-M., and Madec, G.: Influence of numerical schemes on current-topography interactions in 1/4° global ocean simulations, Ocean Sci., 3, 509–524, doi:10.5194/os-3-509-2007, 2007.

Penduff, T., Juza, M., Brodeau, L., Smith, G. C., Barnier, B., Molines, J.-M., Treguier, A.-M., and Madec, G.: Impact of global ocean model resolution on sea-level variability with emphasis on interannual time scales, Ocean Sci., 6, 269–284, doi:10.5194/os-6-269-2010, 2010.

Pohlmann, H., Balmaseda, M., Keenlyside, N., Matei, D., Müller, W., Navarra, A., Rogel, P., and Smith, D.: Atlantic Meridional Overturning Circulation in Decadal Climate Prediction Systems, Unpublished manuscript, 2011.

Robson, J., Sutton, R., Lohmann, K., Smith, D., and Palmer, M. D.: Causes of the Rapid Warming of the North Atlantic ocean in the mid 1990s, J. Climate, doi.:10.1175/JCLI-D-11-00443.1, 2012.

Roullet, G. and Madec, G.: Salt conservation, free surface, and varying levels: a new formulation for ocean general circulation models, J. Geophys. Res., 105, 23927–23942, 2000.

Simmons, A., Uppala S., Dee, D., and Kobayashi, S.: ERA-Interim: New ECMWF reanalysis products from 1989 onwards. ECMWF Newsletter, 110, 25–35, 2007.

Smith, G. C. and Haines, K.: Evaluation of the S(T) assimilation method with the Argo dataset, Q. J. R. Meteor. Soc., 135, 739–756, 2009.

Smith, G. C., Haines, K., Bretherton, D., Gemmell, A., Mugford, R., Stepanov, V., Valdivieso, M., and Zuo, H.: Ocean Reanalysis studies in Reading: Reconstructing Water Mass variability and Transports, Mercator Newsletter, 36, 39–49, 2010.

Stammer, D., Köhl, A., Awaji, T., Balmaseda, M., Behringer, D., Carton, J., Ferry, N., Fischer, A., Fukumori, I., Giese, B., Haines, K., Harrison, E., Heimbach, P., Kamachi, M., Keppenne, C., Lee, T., Masina, S., Menemenlis, D., Ponte, R., Remy, E., Rienecker, M., Rosati, A., Schröter, J., Smith, D., Weaver, A., Wunsch, C., and Xue, Y.: Ocean Information Provided through Ensemble Ocean Syntheses in: Proceedings of OceanObs'09: Sustained Ocean Observations and Information for Society (Vol. 2), Venice, Italy, 21–25 September 2009, edited by: Hall, J., Harrison, D. E., and Stammer, D., ESA Publication WPP-306, 2010.

Stepanov, V., Haines, K., and Smith, G. C.: Assimilation of Rapid Array data into an ocean model, Q. J. Roy. Meteror. Soc., in press., 2012.

Trenberth, K. E., Fasullo, J. T., and Mackaro, J.: Atmospheric moisture transports from ocean to land and global energy flows in Reanalyses, J. Climate, 24, 4907–4924, doi:10.1175/2011JCLI4171.1, 2011.

Troccoli, A. and Haines, K.: Use of the Temperature-Salinity relation in a data assimilation context, J. Atmos. Ocean Tech., 16, 2011–2025, 1999.

Valdivieso, M. and Haines, K.: MyOcean Validation Report (ScVR) for V1 Reprocessed Analysis and Reanalysis. GMES Marine Core Services Technical Report WP04-GLO-U-Reading, 2011.

Wijffels, S.: Ocean transport of fresh water, in: Ocean Circulation and Climate, edited by: Siedler, G., Church, J., and Gould, J., Academic Press, 475–488, 2001.

Wong, T., Stackhouse Jr, P. W., Kratz, D. P., Wilber, A. C.: Earth radiation 283 budget at top-of atmosphere, in: State of the Climate in 2008, B. Am. Meteor. Soc., 90, S33–S34, 2009.

Yu, L., Jin, X., and Weller, R. A.: Multidecade Global Flux Datasets from Objectively Analyzed Air-Sea Fluxes (OAFlux) Project: Latent and Sensible Heat Fluxes, Ocean Evaporation, and Related Surface Meteorological Variables, Woods Hole Oceanographic Institution, OAFlux Project Technical Report, OA-2008-01, January 2008, 2008.

Zheng, Y. and Giese, B. S.: Ocean heat transport in Simple Ocean Data Assimilation: Structure and mechanisms, J. Geophys. Res., 114, C11009, doi:10.1029/2008JC005190, 2009.

Zuo, H. R. I., Mugford, R. I., Haines, K., and Smith, G. C.: Assimilation impacts on Arctic Ocean circulation, heat and freshwater, Ocean Modell., 40, 147–163, doi:10.1016/j.ocemod.2011.08.008, 2011.